

INFLUENCE OF GRAVITY FORCE ON THE INDENTATION OF A COULOMB PLASTIC BY A WEDGE

Miloš Kojić and J. B. Cheatham, Jr.

Introduction

The influence of gravity force on plasticity of Coulomb materials has been considered by several authors. De Jong [1] [2] developed a graphical method and applied it to the solution of the plane indentation problem of a ponderable soil, and Jenike [3] analyzed the flow of bulk materials induced by gravity. Cox [4] formulated a numerical method for the solution of problems involving axially-symmetric and plane plastic deformation of a Coulomb material under the influence of gravity and applied the method to analyze indentation by both an axially-symmetric punch and a plane flat punch. Spenser [5] developed a perturbation method, as an analytical method, and used it to illustrate the influence of gravity on the indentation of a soil by a plane flat punch. Pariseau [6] analyzed gravity induced flow of a granular material in an ore pass as plastic deformation of a Coulomb material; he compared his experimental results with numerical values obtained by an integration along the stress characteristics.

From the results of the above mentioned authors, it can be concluded that gravity force can have an important influence on plasticity solutions for Coulomb materials. Numerical method, developed by Cox, Eason and Hopkins [7] will be applied here to the solution of the plane indentation of a Coulomb material by a wedge, taking into account gravity force. This problem does not appear to have been solved previously.

Solutions of the problem

Suppose that a wedge as shown in Fig. 1a with half of the wedge angle equal to α_w^* is penetrating a semi-infinite surface of a ponderable** soil. Pressure on the surface is a prescribed function, $p_0(x)$ and there are no tangential stresses acting on the surface. The plane of deformation is x, y . The depth of penetration is denoted by $h(ft)$ and the characteristic length, which will be used for the dimensionless solution, is L . From Fig. 1 it follows that

$$(1) \quad h = L \cos \alpha_w.$$

* α_w will be called the wedge angle

** Gravity of material taken into account

It is assumed that there is no friction on the wedge surfaces.

The penetrated material is taken to be a Coulomb material so that at yielding the Coulomb yield criterion in the form



Figure 1(a) shows a slip line field for indentation by a wedge. The wedge is shown with its apex at the origin of a coordinate system (x, y). The slip lines are represented by a series of straight lines forming a fan-like pattern. Points A, B, C, D, E, F, G, H, I, J, K, L, M, N, O, P, Q, R, S, T, U, V, W, X, Y, Z are marked on the slip lines. Figure 1(b) shows a Mohr circle for stress states on the wedge surface. The circle is plotted in the τ - σ plane. The horizontal axis is σ and the vertical axis is τ . The circle is centered on the σ axis. Two straight lines, labeled I and II, form an envelope to the Mohr circles. The angle between the σ axis and line I is β , and the angle between the σ axis and line II is $\beta + \Phi$. The angle between lines I and II is Φ .

$$(2) \quad \left[\left(\frac{\bar{\sigma}_x - \bar{\sigma}_y}{2} \right)^2 + \bar{\tau}_{xy}^2 \right]^{\frac{1}{2}} - \frac{\bar{\sigma}_x + \bar{\sigma}_y}{2} \sin \Phi - c \cdot \cos \Phi = 0$$

is satisfied. $\bar{\sigma}_x$ and $\bar{\sigma}_y$ are the normal stresses (compression positive), $\bar{\tau}_{xy}$ is the shear stress, Φ is the angle of internal friction and c is the cohesion. Bars over the notation for stresses indicate that stresses are dimensional. The two straight lines in the τ - σ plane of Fig. 1b that form an envelope to the Mohr circles represent equation (2) graphically.

Equilibrium equations are

$$(3) \quad \frac{\partial \bar{\sigma}_x}{\partial x} + \frac{\partial \bar{\tau}_{xy}}{\partial y} = 0 \quad \frac{\partial \bar{\tau}_{xy}}{\partial x} + \frac{\partial \bar{\sigma}_y}{\partial y} + \bar{\gamma} = 0$$

Figure 1 (a) Slip line field for indentation by wedge (body force neglected) (b) Mohr circle for stress states on the wedge surface

where \bar{x} and \bar{y} are dimensional coordinate, and $\bar{\gamma}$ is weight of material per unit volume.

Dimensionless stresses σ_x , σ_y and τ , dimensionless ordinates x and y , and dimensionless body force γ are introduced by the following relations:

$$(4) \quad \sigma_x = \frac{\bar{\sigma}_x}{c} \quad \sigma_y = \frac{\bar{\sigma}_y}{c} \quad \tau_{xy} = \frac{\bar{\tau}_{xy}}{c} \quad x = \frac{\bar{x}}{L} \quad y = \frac{\bar{y}}{L} = -z \quad \gamma = \frac{\bar{\gamma}L}{c}$$

The yield condition given by equation (2) is satisfied if stresses satisfy the relations

$$(5) \quad \begin{aligned} \sigma_x &= \sigma [1 + \sin \Phi \sin (2\beta + \Phi)] - \cot \Phi \\ \sigma_y &= \sigma [1 - \sin \Phi \sin (2\beta + \Phi)] - \cot \Phi \\ \tau_{xy} &= -\sigma \sin \Phi \cos (2\beta + \Phi) \end{aligned}$$

where the mean stress σ is given by

$$(6) \quad \sigma = \frac{\sigma_x + \sigma_y}{2} + \cot \Phi.$$

Substituting equations (5) into the equilibrium equations gives two partial differential equations involving variables σ and β that can be transformed into the characteristic form. (See for example reference [8]). The equations of the stress characteristics and the relations along the characteristic are

$$(7) \quad \frac{dy}{dx} = \tan \beta \quad \text{I} \quad \frac{dy}{dx} = \cot (\beta + \Phi) \quad \text{II}$$

$$(8) \quad \begin{aligned} \frac{\partial \sigma}{\partial s_1} + 2\sigma \tan \Phi \frac{\partial \beta}{\partial s_1} &= -\frac{\gamma}{\cos \Phi} \sin(\beta + \Phi) \quad \text{along I} \\ \frac{\partial \sigma}{\partial s_2} - 2\sigma \tan \Phi \frac{\partial \beta}{\partial s_2} &= \frac{\gamma}{\cos \Phi} \cos \beta \quad \text{along II} \end{aligned}$$

where β is the angle of the first characteristic, and s_1 and s_2 are dimensionless curvilinear coordinates along the first and second characteristic shown in Fig. 2. Introduce, as was done in reference [7], the variable ω by the relation

$$(9) \quad \omega = \cot \Phi \ln \sigma$$

so that equations (8) can be written in the following form:

$$(10) \quad \begin{aligned} d\omega + 2d\beta &= -\frac{\gamma}{\sin \Phi} \sin(\beta + \Phi) e^{-\omega \tan \Phi} ds_1 \quad \text{along I} \\ d\omega - 2d\beta &= \frac{\gamma}{\sin \Phi} \cos \beta e^{-\omega \tan \Phi} ds_2 \quad \text{along II} \end{aligned}$$

The first approximation of point R at the intersection of two stress characteristics is denoted by R_1 . Then, according to the geometry shown in Fig. 2 and from equations (7) and (10), it follows that

$$(11) \quad \begin{aligned} x &= \frac{1}{\tan \beta_P + \cot(\beta_Q + \Phi)} [x_P \tan \beta_P + x_Q \cot(\beta_Q + \Phi) + z_P - z_Q] \\ z &= \frac{1}{\tan \beta_P + \cot(\beta_Q + \Phi)} [(x_P - x_Q) \tan \beta_P \cot(\beta_Q + \Phi) + z_P \cot(\beta_Q + \Phi) \\ &\quad + z_Q \tan \beta_P] \end{aligned}$$

$$(12) \quad \begin{aligned} \omega &= \frac{\omega_P + \omega_Q}{2} + \beta_P - \beta_Q + \frac{\gamma}{2} \{ [-x + x_P + (z - z_P) \cot \Phi] e^{-\omega_P \tan \Phi} \\ &\quad + [x - x_Q + (z - z_Q) \cot \Phi] e^{-\omega_Q \tan \Phi} \} \end{aligned}$$

$$(13) \quad \begin{aligned} \beta &= \frac{\beta_P + \beta_Q}{2} + \frac{\omega_P - \omega_Q}{4} + \frac{\gamma}{4} \{ [-x + x_P + (z - z_P) \cot \Phi] e^{-\frac{\omega_P + \omega}{2} \tan \Phi} \\ &\quad - [x - x_Q + (z - z_Q) \cot \Phi] e^{-\frac{\omega_Q + \omega}{2} \tan \Phi} \} \end{aligned}$$

where x , z , and ω and β are the first approximations, corresponding to point R_1 , and indices P and Q correspond to values of variables at points P and Q . When the first approximations are obtained, the second approximations can be found as follows:

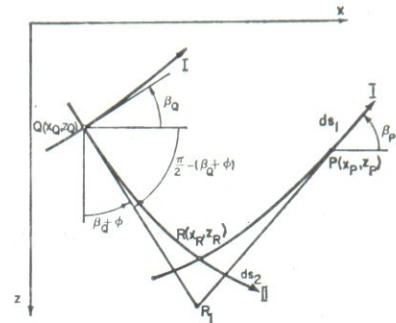


Figure 2. The geometry used for numerical solutions

- (a) in equations (11) replace β_P by $(\beta_P + \beta)/2$ and β_Q by $(\beta_Q + \beta)/2$; and
 (b) substitute the second approximations of x and z into equations (12) and replace

$$e^{-\omega_P \tan \Phi} \quad \text{by} \quad e^{-\frac{\omega_P + \omega}{2}}$$

and

$$e^{-\omega_Q \tan \Phi} \quad \text{by} \quad e^{-\frac{\omega_Q + \omega}{2}}$$

to find the second approximation of ω ; and

- (c) use the second approximations of x , z and ω in equation (13) to obtain the second approximation of β .

The above procedure can be repeated until convergence is obtained. It is considered here that convergence is attained when the difference between the coordinates of points R for two successive approximations is less than 0.1 percent of dx , where dx is the increment along the x axis between two characteristics (length MM_1 in Fig. 1a).

The influence of gravity is neglected at point 0, which is analogous to the conditions accepted for the indentation by a flat punch in references [1], [2], [4], [5], [7], and [8]. The initial stress characteristic MSKT encloses the region in which the influence of gravity is neglected. Although the computer program was written for $p_0(x)$ being a linear function of x , the solutions presented here are for $p_0(x)=0$. The initial dimensionless length is taken to be 0.05.

The lip BOO' is neglected for the sake of simplicity. When the first line I is computed, that line becomes an initial line for the subsequent calculation and so on. The solution of the problem is considered to have been obtained when a computed characteristic crosses the line OA below point A . The line $AK_1S_1B_1$ corresponds to the solution without body force influence.

Stress states along the surface OA are represented in Fig. 1b, from which the following can be obtained:

$$(14) \quad \sigma_N = e^{\omega \tan \Phi} (1 + \sin \Phi) - \cot \Phi$$

where σ_N is the stress at point T normal to the wedge surface.

The dimensionless depth of penetration, H , here called the reduced depth of penetration, is defined in the following way:

$$(15) \quad H = \frac{h\bar{\gamma}}{c}$$

From equations (4) and (15) it follows that

$$(16) \quad \frac{H}{\cos \alpha_W}$$

From the definition of the reduced depth of penetration it follows that it is zero in two cases: (a) when the influence of gravity is neglected, i. e., $\bar{\gamma}/c \approx 0$ and (b) when the depth of penetration is small, i. e., $h \approx 0$.

The integral of σ_N along OA gives the normal force on the wedge:

$$(17) \quad f_N = \int_0^1 \sigma_N dx_T = \frac{F_N}{cL}$$

where x_T is the coordinate on the wedge surface, F_N is the dimensional and f_N is the dimensionless normal force on the wedge surface. Note that f_N is essentially the average normal stress on OA . Define the dimensionless force, f_w , on the wedge by

$$(18) \quad f_w = \frac{F_w}{ch}$$

where F_w is the dimensional wedge force. From equations (1); (17) and (18) it follows that f_w can be expressed as

$$(19) \quad f_w = 2 f_N \tan \alpha_w$$

If $\alpha_w \rightarrow \pi/2$, then

$$\frac{h}{\cos \alpha_w} \rightarrow 1$$

the wedge approaches a flat punch and the force on the punch is

$$(20) \quad f_w = 2 f_N$$

From solutions in dimensionless form the dependence of the wedge force, f_w , on the reduced depth, H , is presented in Fig. 3 for the angle $\Phi=20^\circ$ and in Fig. 4 for $\Phi=30^\circ$. The solutions are obtained for several values of the wedge angle α : 10° , 20° , 45° and 60° . Note that ordinates in Figs. 3 and 4 are logarithmic.

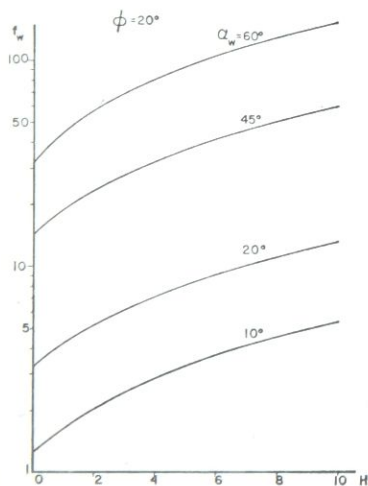


Figure 3. Wedge force as a function of the reduced depth of penetration and wedge angle ($\Phi=20^\circ$)

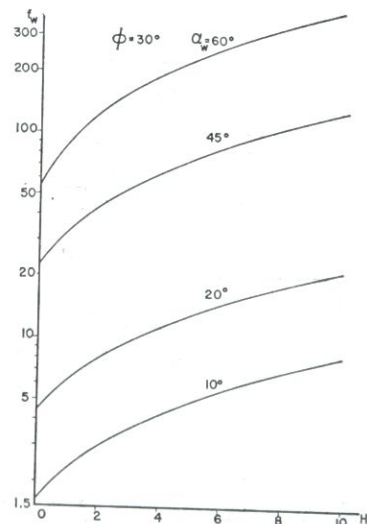


Figure 4. Wedge force as a function of the reduced depth of penetration and wedge angle ($\Phi=30^\circ$)

Figs. 5 and 6 give the normal force (average stress) in terms of the reduced depth, H , and the angle α_w , for materials with $\Phi=20^\circ$ and $\Phi=30^\circ$. It can be seen from these Figures that the average normal pressure changes approximately linearly with H . It should be pointed out the ordinates for $H=0$ (which corresponds to

$\bar{\gamma}/c \approx 0$) in Figs. 3 through 6 represent solutions for the case when the influence of gravity is neglected.

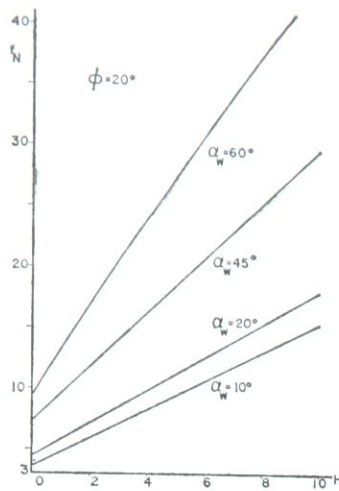


Figure 5. Normal force on the side of wedge as a function of the reduced depth of penetration and wedge angle ($\Phi = 20^\circ$)

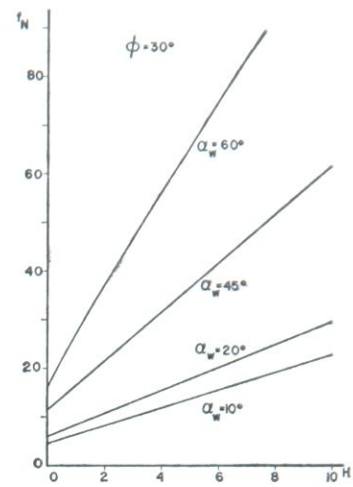


Figure 6. Normal force on the side of wedge as a function of the reduced depth of penetration and wedge angle ($\Phi = 30^\circ$)

Some examples of the computed fields of the stress characteristics are presented in Fig. 7. The dependence of the ratio OB/OA on the reduced depth and the wedge angle is given in Fig. 8. Point B is an intersection of the last computed line I with the x axis and the length OB characterizes the magnitude of the field of plastic deformation. It can be seen from the last two Figures that the magnitude of the field of plastic deformation decreases with and increase of H .

Finally, an example in dimensional form will be solved to illustrate the use of the general, dimensionless solutions. Assume the following values:

$$\begin{aligned} \Phi &= 30^\circ \\ \bar{\gamma} &= 175 \text{ (p/ft}^3\text{)} \\ c &= 5 \text{ (psi)} = 720 \text{ (p/ft}^2\text{)} \end{aligned}$$

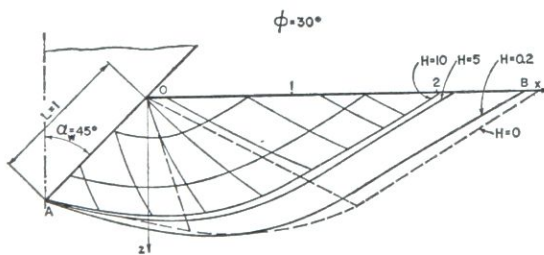


Figure 7. The magnitude of the field plastic deformation for indentation by wedge as a function of the reduced depth of penetration, H

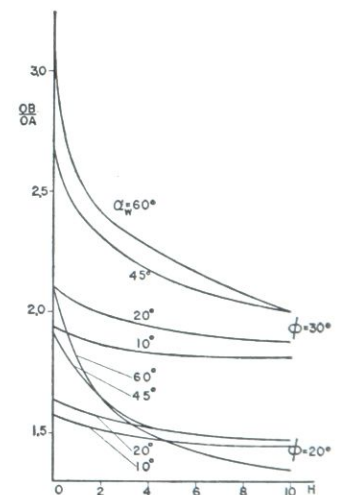


Figure 8. Ratio of the extent of the slip-line field, OB , to the characteristic length, OA , as a function of the reduced depth of penetration and wedge angle

From the above, the ratio $\bar{\gamma}/c$ is

$$(21) \quad \bar{\gamma}/c = 0.243 \text{ (ft}^{-1}\text{)}$$

For every depth of penetration h (ft), the reduced depth, H , can be computed using the relation (21) and for the corresponding α_w the dimensionless force, f_w

can be found from Fig. 4. With the known f_w , the dimensional wedge force, F_w , can be computed from equation (18), i. e.,

$$F_w = f_w ch$$

If the influence of gravity is neglected, the force on the punch is

$$F_w = (f_w)_0 ch$$

where $(f_w)_0$ is f_w for $H=0$. From the last expression, it follows that F_w is a linear function of h since $(f_w)_0$ and c are constants.

The results of the above computation are presented in Fig. 9, where dashed lines correspond to the solution without the influence of gravity. It can be seen from the Figure 9 that the influence of gravity increases with the depth of penetration. This is expected (see results in [4], [5] and [8]) since the body force influence increases with the magnitude of the field of plastic deformation.

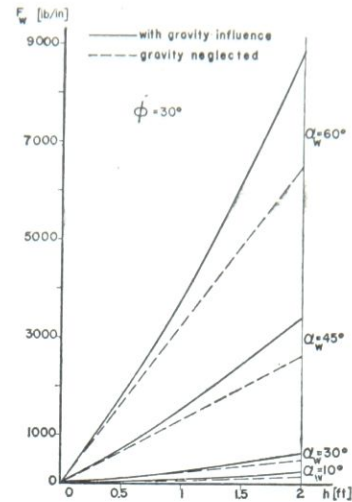


Figure 9. Wedge force [lb/in] as a function of the depth of penetration [ft] and wedge angle

Conclusions

From the results presented, it can be concluded that gravity can have an important influence on the solution of the wedge indentation problem. Analogous to the results obtained for the indentation by a flat punch, it can be seen here that the gravity force increases pressure on the wedge surface and the wedge force. The influence increases with an increase of the depth of penetration and also with an increase of the wedge angle.

Gravity causes the magnitude of the field of plastic deformation to decrease with the relative decrease being greater for larger depths of penetration.

It should be pointed out, finally, that the influence of gravity is greater for material with small cohesion, c . This conclusion is obvious since H increases with a decrease of the cohesion at the same weight per unit volume and the same depth of penetration, h .

NOMENCLATURE

c	Cohesive strength
F_N	Dimensional normal force on wedge
f_N	Dimensionless normal force on wedge
F_w	Dimensional force on wedge
f_w	Dimensionless force on wedge
H	Dimensionless depth of penetration
h	Depth of penetration
L	Characteristic length used for dimensionless solutions
$p_0(x)$	Pressure acting on surface
R, P, Q	Points in physical plane
R_1	First approximation to point R
s_1, s_2	Dimensionless curvilinear coordinates along first and second characteristics
\bar{x}, \bar{y}	Dimensionless coordinates
x, y	Dimensional coordinates
$z = -y$	
α_w	Half angle of wedge
β	Angle of first characteristic

β_P, β_Q	Values of β at points P and Q
γ	Dimensionless body force
γ	Weight of material per unit volume
Φ	Angle of internal friction
τ_{xy}	Dimensionless shear stress
τ_{xy}	Shear stress
σ_x, σ_y	Dimensionless normal stresses
σ_x, σ_y	Normal stresses (compression positive)
σ	Mean stress
$\omega = \cot \omega \ln \sigma$	
ω_P, ω_Q	Values of ω at points P and Q

REFERENCES

- [1] G. De Josselin De Jong, *Grapfische Bepaling van Glijlijin Patronen in de Grondmechanica*, De Ingenieur, v. 69, No. 29, pp. 61—65, 1957.
- [2] G. De Josselin De Jong, *Statics and Kinematics in the Failable Zone of a Granular Material*, Waltman, Delft, 1959.
- [3] A. Jenike, *Gravity Flow of Bulk Solids*, Bull. of Univ. of Utah, v. 52, No. 29, 1961.
- [4] A. D. Cox, *Axially-Symmetric Plastic Deformation in Soils. II. Indentation of Ponderable Soils*, J. Mech. Sci., v. 4, pp. 371—380, 1962.
- [5] A. J. M. Spenser, *Perturbation Methods in Plasticity-III: Plane Strain of Ideal Soils and Plastic Solids with Body Forces*, J. Mech. Phys. Solids, v. 10, pp. 165—177, 1962.
- [6] W. G. Pariseau, *The Gravity Indiced Movement of Materials in Ore Passes Analyzed as a Problem in Coulomb Plasticity*, Ph. D. Thesis, Univ. of Minnesota, 1966.
- [7] A. D. Cox, G. Eason and H. G. Hopkins, *Axially-Symmetric Plastic Deformation in Soils*, Phil. Trans. Roy. Soc. London, v. 254, No. 1036, pp. 1—45, 1961.
- [8] M. Kojić, *Influence of Fluid Pressure Gradient on Plasticity of Porous Media*, Ph. D. Thesis, Rice University, Houston, 1972.

ACKNOWLEDGEMENT

The authors wish to acknowledge their appreciation to the American Petroleum Institute Project 67F, to the Humble Oil Education Foundation and to Schlumberger Well Services for support of the work reported here.

L'INFLUENCE DE LA FORCE DE GRAVITÉ SUR L'INDENTATION DE COULOMB PLASTIQUE AU MOYEN DE LA CLAVETTE

M. Kojić, J. B. Cheatham, Jr.

Résumé

L'influence de la force de gravité sur l'indentation de Coulomb plastique au moyen de la clavette est analysée à l'aide de la méthode numérique. Les solutions sont obtenues à la forme non — dimensionale pour plusieurs angles de clavette et pour deux angles de friction interne. Un exemple est donné à la forme dimensionale.

(Received June 30, 1975)

Miloš Kojić
Mašinski Fakultet 3400 Kragujevac, Yugoslavia
J. B. Cheatham Jr.
Professor of Mechanical Engineering
Rice University, Houston, Texas